

# Design and Measurement of a 600 GHz Micromachined Horn Antenna Manufactured by Combined DRIE and KOH-Etching of Silicon

Stephan Biber<sup>1</sup>, Axel Murk<sup>2</sup>, Lorenz-Peter Schmidt<sup>1</sup>, Niklaus Kämpfer<sup>2</sup>

**Abstract**—We present a detailed discussion of a manufacturing process used for silicon-micromachining of horn antennas for submillimeter wave applications. The developed process was applied to the machining of an octagonal horn antenna for 600 GHz and can be scaled for frequencies up to 3 THz. The antenna geometry was optimized for maximum coupling to a Gaussian beam using the commercial simulation tool "Microwave Studio". It was found that maximum Gaussian coupling can be up to 86%. Measurement results for an E-plane and an H-plane scan of the antenna pattern show good agreement with simulation results. The process involves a deep reactive ion etching process (DRIE) creating rectangular trenches which form the waveguide (overall size of 420x210  $\mu\text{m}$ ) and open the antenna in the E-plane. A KOH-etching process is applied on the bottom of the trenches formed in the preceding DRIE process. This wet etching process with a depth of 320  $\mu\text{m}$  allowed to open the antenna aperture in the H-plane.

**Index Terms**—antenna-design, THz-technology, micromachining, silicon-technology, quasi-optics

## I. INTRODUCTION

Antennas are an integral part of quasi-optical systems at THz-frequencies. Many applications require antennas with high coupling efficiency to a Gaussian beam. Horn-antennas as well as lens antennas are mostly used for this purpose. As the dimensions of the antennas become very small at submillimeter wave frequencies, conventional manufacturing processes such as milling and drilling etc. hardly enable to manufacture the complex structures with the desired tolerances.

The application of micromachining techniques for the manufacturing of antennas is a new challenge for the available micromachining technologies, because antennas usually have complex geometries. It is difficult to achieve an antenna aperture similar to a pyramidal or conical horn using a micromachining process because this requires a rectangular waveguide to be opened in three directions. Antennas for THz-mixers are usually optimized for maximum coupling between a fundamental mode Gaussian beam and the antenna. Therefore the geometry of the antenna has to be adapted to the circular pattern of the Gaussian beam.

Best coupling coefficients can be obtained by circular corrugated feed horns with an integrated circular to rectangular waveguide transition [1], [2], but these structures require high geometrical flexibility during the manufacturing process. Rectangular horn antennas [3], diagonal horn antennas [4] as

well as hexagonal horn antennas are widely used because of their simple geometry and comparatively large coupling efficiencies of up to 88%. Another approach to integrate both rectangular structures for waveguides and antennas in the same micro-machining process is the application of different etching techniques in silicon. Hesler et al. have demonstrated an octagonal horn antenna based on SU-8 for the waveguide layer and wet etching of 100-oriented silicon [5] for widening the antenna aperture. We propose the machining of an antenna, purely based on silicon machining techniques, replacing the SU-8 process with a dry-etching technique. The antenna can be assembled from two symmetrical split-block halves, cutting the waveguide in the E-plane.

One major advantage of silicon micromachining technology compared to conventional techniques is its capability to manufacture many components in one production process. With the antenna design described below, more than 40 antennas can be machined on one single silicon wafer (with 100 mm diameter). The silicon micromachining technology allows not only the production of many isolated components. Various different components can be machined quasi-monolithically for an advanced production of THz-circuits and systems such as receiver arrays for imaging applications.

This paper will discuss the special issues related to the manufacturing process and the combination of DRIE and KOH-etching. We will present a detailed examination of the coupling efficiency and its dependence on the geometry of the antenna. A comparison between simulation and measurement results for the antenna pattern at 600 GHz will conclude the paper.

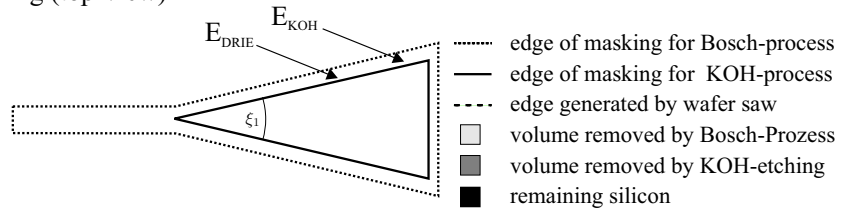
## II. THE MICROMACHINING PROCESS

The manufacturing process described in Fig. 1 shows the major steps for the production of the antenna and the necessary masking of the silicon structures. In step 1, a DRIE-process ("Bosch-process" [6]) is used to form one half of the waveguide and to form the antenna by opening the waveguide in the E-plane. The waveguides used for 600 GHz have dimensions of  $a = 420 \mu\text{m}$  and  $b = 210 \mu\text{m}$ . Therefore an etching depth of  $t_{DRIE} = a/2 = 210 \mu\text{m}$  is required. As such an antenna would be an E-sectorial horn antenna with a rather poor Gaussian coupling efficiency, an enhanced opening of the antenna aperture in the H-plane is required. This is accomplished in step 2 by using a KOH-etching process. The KOH-etching process is a wet etching process which allows

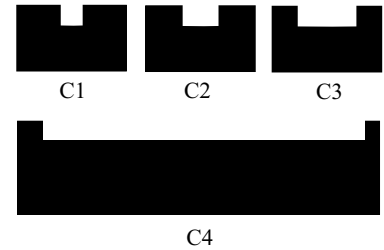
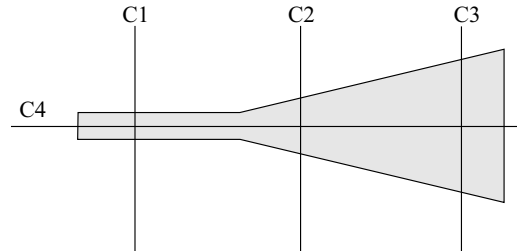
<sup>1</sup>Institute for Microwave Technology, University of Erlangen-Nuremberg, Germany

<sup>2</sup>University of Bern, Institute of Applied Physics, Switzerland

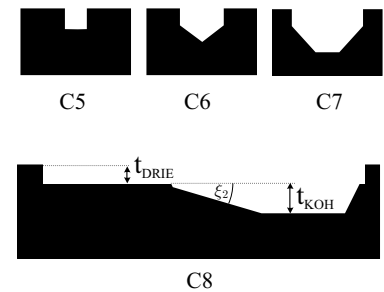
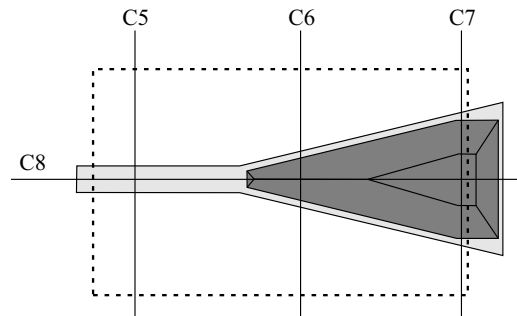
Masking (top-view)



Bosch-process (top-view)



KOH-process (top-view)



final mounting of the antenna (side-view)

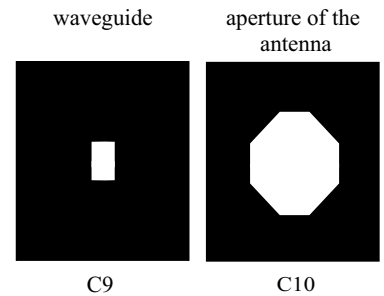
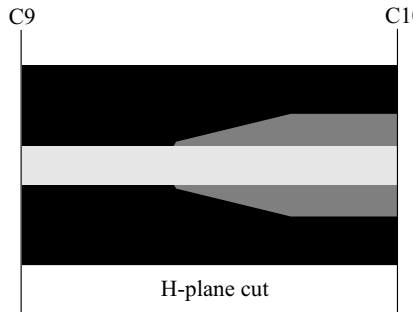


Fig. 1. Overview on the process. Left: top-view on the structures, right: respective cut-views (C1-C3, C5-C7, C9-C10) and (C4, C8).

strongly anisotropic etching of silicon crystals [7], [8]. With the 100-wafers used for this process, it is possible to use the 111-planes of the silicon crystal as etch-stop layers, because the etching rate in 111-direction is 400 times slower than it is in the 100 -direction.

Several difficulties have to be overcome in order to successfully complete the micromachining process: The necessary dry etching depth has to be achieved in one etching step, which requires the deposition and structuring of a thick, chemically robust masking layer. In order to combine the structures generated by the DRIE process with the KOH-etching process, two technological problems have to be solved:

First the complex topology generated by the DRIE process has to be completely masked to ensure that the KOH-etching process can only etch the silicon in the desired, triangular region shown in Fig. 1a. Second, photolithographic mask transfer with a large distance  $t_{DRIE}$  between the mask and the substrate has to be accomplished successfully.

The wafers used for the process have a thickness of  $1325 \mu\text{m}$  and a diameter of 100 mm. Comparatively thick wafers are necessary to ensure mechanical stability of the device even after the completion of the etching process, which is generating deep trenches in the silicon. Before starting the "Bosch-process" for the etching of the waveguide and the opening of

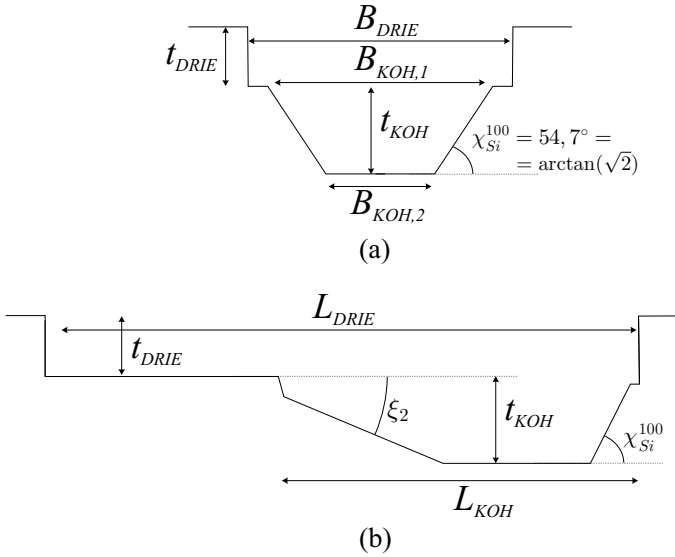


Fig. 2. Dimensions: (a) one split-block half of the antenna, front-view on the aperture, (b) cut through the side-view of the antenna

the antenna in the  $E$ -plane, the mask for this process has to be deposited and structured on the wafer. As this mask has to be very thick in order to withstand an etching depth of  $210 \mu\text{m}$  it was deposited in three steps. The first  $\text{SiO}_2$  layer was grown thermally, the second  $\text{SiO}_2$  layer was deposited using a chemical vapour deposition process and finally the third layer consisting of photoresist was spun on top. This gives an overall thickness of the mask of  $3 \mu\text{m}$ .

After the completion of step 1 (Fig. 1b), the whole structure was coated with an  $\text{SiO}_2$  layer using a thermal oxidation process and then coated with photoresist. In order to have a complete coating of the topology - also on the vertical sidewalls generated by the DRIE process - the photoresist was not spun but sprayed on the wafer. The difficulty to illuminate the photoresist on the bottom of the  $210\mu\text{m}$  deep trenches could be overcome by using a projection aligner. The projection aligner allows a mask transfer with a large distance between the mask and the wafer.

After the completion of the etching processes, the antennas are diced using a wafer-saw (Fig. 1c) and then coated with a  $2 \mu\text{m}$  thick gold layer providing high electrical conductivity. In the final step 3 (Fig. 1d), the two split-block halves are assembled in a conventionally machined brass mount.

### III. DESIGN AND OPTIMIZATION OF THE ANTENNA

The available etching technologies and the limitations given by the principal planes of the silicon crystal limit the possible geometries available for this antenna design. Figure 2 shows the most important dimensions of the antenna.

The opening angle of the antenna  $\xi_1$  is given by the parameters  $B_{\text{KOH}}$  and  $L_{\text{KOH}}$  due to:

$$\xi_1 = \arctan\left(\frac{B_{\text{KOH}}}{2L_{\text{KOH}}}\right) . \quad (1)$$

Together with the geometry of the silicon crystal, this yields:

$$\xi_2 = \arctan\left(\tan\left(\frac{\xi_1}{2}\right) \cdot \tan(\chi_{\text{Si}}^{100})\right) , \quad (2)$$

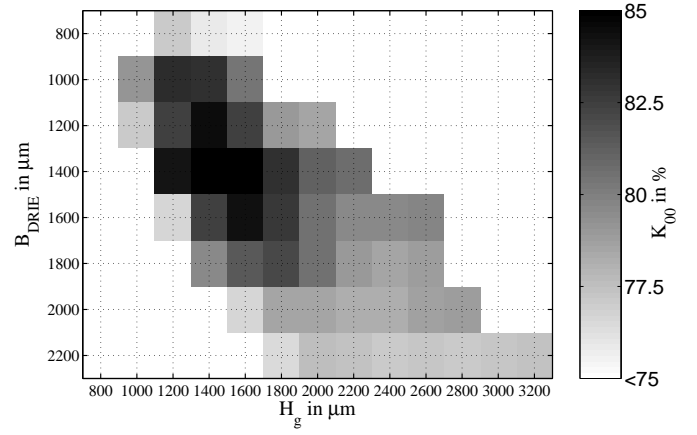


Fig. 3. Coupling efficiency  $K_{00}$  of the antenna with a fundamental mode Gaussian beam as a function of the antenna geometry.  $B_{\text{DRIE}}$  is the aperture width in the  $E$ -plane,  $H_g$  the width in the  $H$ -plane.

with the angle  $\chi_{\text{Si}}^{100}$  between the 100- and the 111-plane of the silicon crystal:

$$\chi_{\text{Si}}^{100} = 54.74^\circ . \quad (3)$$

The depth of the KOH-etching process  $t_{\text{KOH}}$  is limited by the width  $B_{\text{KOH},1}$  of the structures on the wafer surface:

$$t_{\text{KOH}} < t_{\text{KOH}}^{\text{max}} = \frac{B_{\text{KOH},1}}{2} \tan(\chi_{\text{Si}}^{100}) . \quad (4)$$

If the etching process is stopped before reaching the maximum depth  $t_{\text{KOH}}^{\text{max}}$ , the width  $B_{\text{KOH},2}$  is given by:

$$B_{\text{KOH},2} = B_{\text{KOH},1} - \frac{2t_{\text{KOH}}}{\tan(\chi_{\text{Si}}^{100})} . \quad (5)$$

Equations 1 - 5 define the mutual dependencies of the geometry of the antenna after the completion of the etching process.

In order to maximize the Gaussian coupling to this antenna, a model of the antenna was implemented in "Microwave Studio" (MWS). The electric fields calculated by MWS were exported to MATLAB where the maximum coupling coefficient  $K_{00}$  between the antenna and a fundamental mode Gaussian beam was calculated for each antenna design. The major antenna parameters examined in a comprehensive parameter study are the diameter of the aperture in the  $E$ - and in the  $H$ -plane. The diameter of the aperture in the  $E$ -plane is defined by  $B_{\text{DRIE}}$  while it is defined in the  $H$ -plane by:

$$H_g = 2 \cdot (t_{\text{DRIE}} + t_{\text{KOH}}) , \quad (6)$$

$$t_{\text{DRIE}} = 210 \mu\text{m} . \quad (7)$$

The results of this parameter study, including an analysis of over 60 different antenna designs, are summarized in Fig. 3. This Figure shows that the maximum coupling to a Gaussian beam with a beam radius of  $w_0 = \lambda_0 = 500 \mu\text{m}$  can be achieved for a horn aperture with  $B_{\text{DRIE}} = 1200 \mu\text{m}$  and  $H_g = 1600 \mu\text{m}$ . The simulated coupling efficiency for this antenna yields  $K_{00}^{\text{max}} = 86\%$ . As the length of the antenna  $L_{\text{KOH}}$  does not have a significant influence on the coupling efficiency for  $L_{\text{KOH}} = 8000\text{--}14000 \mu\text{m}$ , the simulations presented here are based on  $L_{\text{KOH}} = 10000 \mu\text{m}$ .

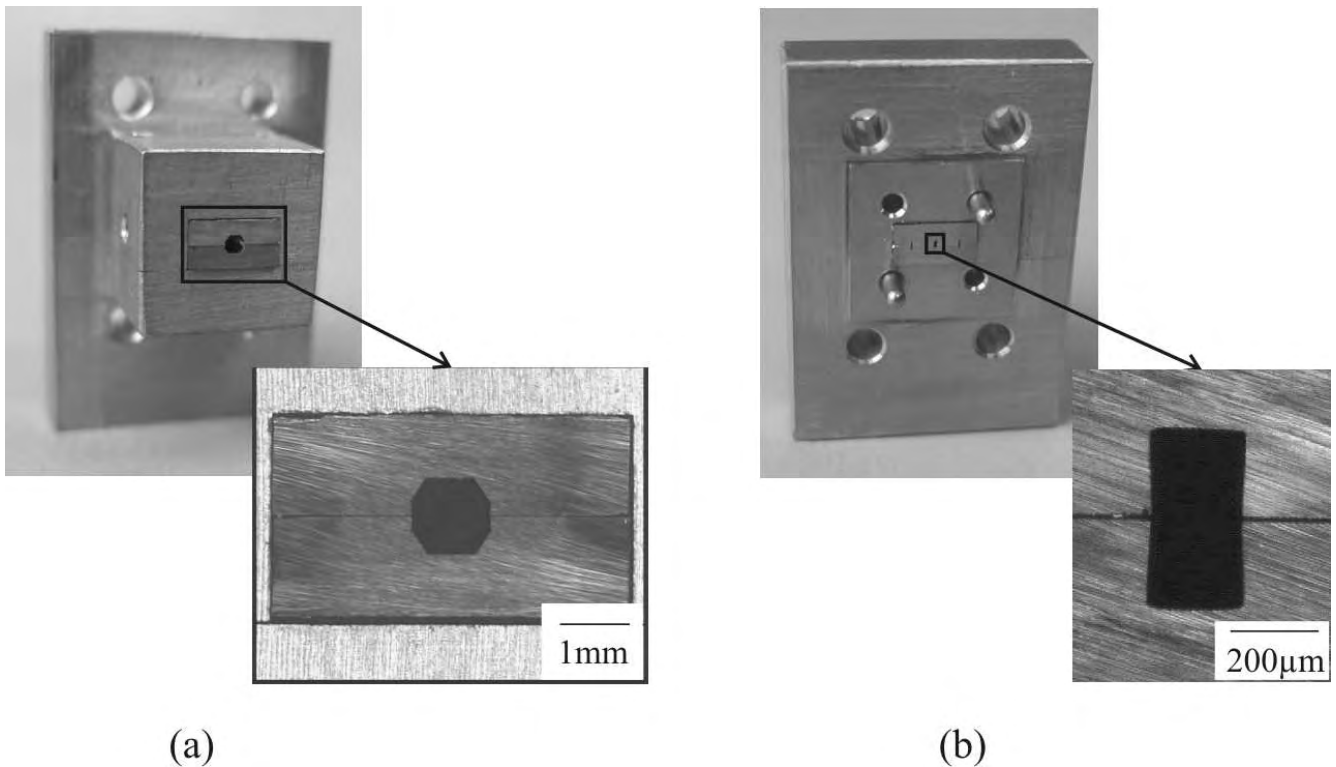


Fig. 4. Antenna assembled in brass-mount; (a) front-view on antenna aperture (b) waveguide input with flange and dowel pins

As the optimum antenna geometry with an  $H$ -plane diameter of  $H_g = 1600 \mu\text{m}$  requires a rather large KOH-etching depth of  $t_{\text{KOH}} = 590 \mu\text{m}$ , we decided to produce a slightly smaller aperture with  $H_g = 1300 \mu\text{m}$  and  $B_{\text{DRIE}} = 1100 \mu\text{m}$ . This design only requires an etching depth of  $t_{\text{KOH}} = 450 \mu\text{m}$  and still provides a coupling efficiency of  $K_{00} = 85\%$  which is just 1% less than the maximum achievable efficiency.

#### IV. RESULTS OF THE MICROMACHING PROCESS

The desired etching depth for the DRIE-process of  $t_{\text{DRIE}} = 210 \mu\text{m}$  could be achieved with negligible variations of less than  $4 \mu\text{m}$ . Larger variations from the original goal had to be accepted for the KOH-etching depth  $t_{\text{KOH}}$ . A critical parameter in the described process is the underetching of the edges  $E_{\text{KOH}}$  (see Fig. 1a) which are not parallel to the principal planes of the silicon crystal. If the underetching proceeds beyond the point, where the edges  $E_{\text{KOH}}$  and  $E_{\text{DRIE}}$  coincide, the structure would be destroyed because the new crystal planes which would be opened are etched at a very high rate by the KOH-solution.

Although the underetching rate can be calculated from the etching rate along the principal planes [9], in the actual process it can only be controlled by measuring the distance between the edges  $E_{\text{KOH}}$  and  $E_{\text{DRIE}}$  using a microscope. The etching process was stopped, as soon as both edges could not be distinguished anymore. As both edges are separated vertically by  $t_{\text{DRIE}} = 210 \mu\text{m}$  it is very difficult to precisely determine the moment when both edges coincide. Therefore the etching process was stopped slightly earlier than desired in order to

prevent the destruction of the structure. This led to an overall KOH-etching depth of  $t_{\text{KOH}} = 330 \mu\text{m}$ . Although this is significantly less than the desired etching depth of  $450 \mu\text{m}$  it has only minor impact on the coupling efficiency  $K_{00}$ . From Fig. 3 it can be seen that the machined antenna still provides a coupling efficiency of  $K_{00} = 81\%$ . The readily assembled antenna has an octagonal aperture with  $1080 \mu\text{m}$  width in the  $E$ -plane and  $1074 \mu\text{m}$  in the  $H$ -plane and is shown in Fig. 4.

#### V. MEASUREMENT RESULTS

For the characterization of the antenna, the far-field antenna pattern  $C_s$  was measured in the  $E$ - and in the  $H$ -plane at a frequency of 600 GHz. For the two different orientations, the antenna under test was mounted on a rotation stage with its aperture close to the rotational axis. The antenna was connected to a harmonic Schottky diode mixer which was pumped at 100 GHz by a Gunn diode local oscillator. A similar Gunn oscillator followed by a  $\times 6$  multiplier and a 550 GHz high-pass filter was used as signal source mounted in a distance of about 300 mm from the rotation stage. Both oscillators were phase-locked to the same reference signal. The down-converted signal at an intermediate frequency of 59 MHz was analyzed in amplitude and phase with an ABmm vector network analyzer. The available dynamic range in this configuration is more than 50 dB. In order to reduce the effect of standing waves between the two horn antennas the measurements in each plane were repeated four times after an axial  $\lambda/4$  shift of the signal source. The surrounding areas in the field of view of the antenna were covered with microwave

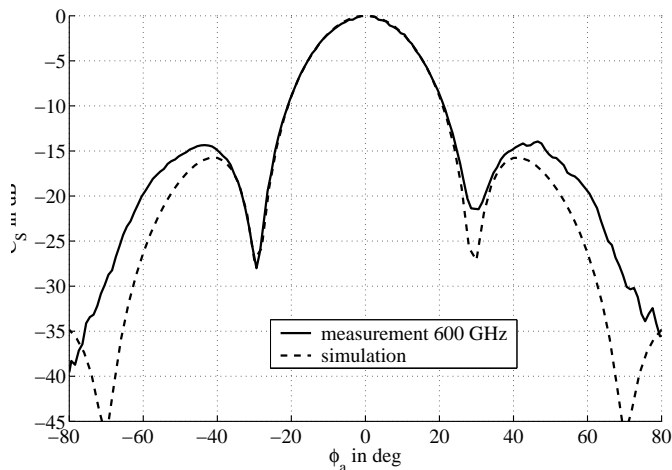


Fig. 5. Antenna pattern in the  $E$ -plane: Comparison of measurement results at 600 GHz with simulation results based on "Microwave Studio".

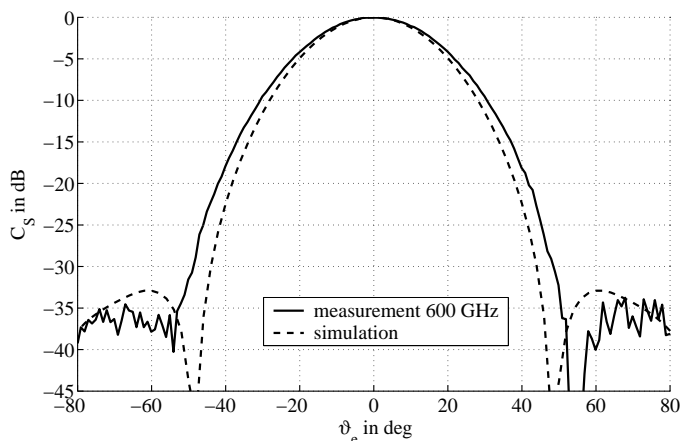


Fig. 6. Antenna pattern in the  $H$ -plane: Comparison of measurement results at 600 GHz with simulation results based on "Microwave Studio".

absorbing materials (TK-RAM and Eccorsob) to prevent other multi-path signals which could not be corrected with the phase-shifting technique.

The  $E$ -plane scan was accomplished by scanning the azimuth angle  $\Phi_a$ , while the  $H$ -plane scan was accomplished by scanning the elevation angle  $\vartheta_e$  with the main lobe of the antenna oriented in the direction of  $\vartheta_e = 90^\circ$ .

Fig. 5 and 6 show the comparison between the simulated and measured antenna pattern. The antenna parameters used in the simulations are based on the geometry of the antennas after the completion of the micromachining process and the assembly of both split-block halves ( $B_{DRIE} = 1080 \mu\text{m}$ ,  $H_g = 1074 \mu\text{m}$ ).

A very good agreement between the simulated and the measured results can be observed for the  $E$ -plane. The maximum measured side lobe level in the  $E$ -plane is with -14.5 dB only about 1 dB higher than predicted by the simulation. The location of the minima in the antenna pattern at  $\Phi_a = \pm 29.5^\circ$  could also be verified very precisely. The 3-dB-beamwidth of the main lobe of the antenna equals  $24.5^\circ$ .

A comparison of simulated and measured data in the

$H$ -plane shows that the measured beamwidth is larger than the beamwidth given by the simulation. As the difference between the measured 3-dB-beamwidth of  $33.6^\circ$  and the simulated beamwidth of  $31.6^\circ$  is only  $2^\circ$ , this effect is only of minor importance for the overall performance of the antenna. The sidelobe level in the  $H$ -plane is -34 dB. This is still significantly above the noise floor of the measurement system.

A precise calculation of the coupling efficiency  $K_{00}$  from measurement data requires a complete hemispherical scan of the antenna, which would be very time-consuming. As a good agreement between simulation and measurement could be observed in the principal planes of the antenna, a complete hemispherical scan would not significantly add new information. The good agreement allows to conclude that the coupling efficiency  $K_{00} \approx 80\%$  calculated for the antenna model in MWS also holds for the real antenna.

## VI. DISCUSSION AND OUTLOOK

A micromachining technology for the manufacturing of an octagonal horn antenna with high coupling to a Gaussian beam has been presented. Coupling coefficients for more than 60 antenna geometries have been calculated using the field simulator MicrowaveStudio. The maximum coupling coefficient found was  $K_{00}^{max} = 86\%$ . Special questions concerning the combination of the DRIE- and the KOH-etching process such as underetching effects and masking of complex topologies have been addressed. With the measurement results at 600 GHz being in good agreement with the simulation, a coupling efficiency of  $K_{00} \approx 80\%$  could be verified. The antenna has been successfully used as an input of a conventionally machined GaAs Schottky-diode mixer with a conversion loss as low as 9.5 dB [10].

## ACKNOWLEDGMENT

We are very grateful to the German Research Foundation ("Deutsche Forschungsgemeinschaft") for partially funding this project. The work at IAP in Bern was supported by the Swiss National Science Foundation under the grant 200020-100167. Special thanks to Gudrun Rattmann and Sven Berberich from "Fraunhofer Institute for Integrated Systems and Device Technology" (IISB) and to Theo Hartmann from Nanoworld GmbH. Micromachining of the antennas would not have been possible without their help and the availability of the machining technologies in the clean-room facility of IISB on the campus of the University of Erlangen-Nuremberg.

## REFERENCES

- [1] P. F. Goldsmith, "Quasi-optical techniques," *Proceedings of the IEEE*, vol. 80, pp. 1729-1747, November 1992.
- [2] P. H. Siegel, R. P. Smith, M. C. Gaidis, and S. C. Martin, "2.5 THz GaAs monolithic membrane-diode mixer," *IEEE Transactions on Microwave Theory and Techniques*, vol. 47, pp. 596-604, May 1999.
- [3] F. Maiwald, J. C. Pearson, J. S. Ward, E. Schlecht, G. Chattopadhyay, J. Gill, R. Ferber, R. Tsang, R. Lin, A. Peralta, B. Finamore, W. Chun, J. J. Baker, R. J. Dengler, H. Javadi, P. Siegel, and I. Mehdi, "Solid-state sources for space applications," in *Conference Digest of the 29th Int. Conf. On Infrared and Millimeter Waves, Karlsruhe, Deutschland* (T. M. and W. W., eds.), 2004.

- [4] J. F. Johansson and N. D. Whyborn, "The diagonal horn as a sub-millimeter wave antenna," *IEEE Trans. Microwave Theory and Techniques*, vol. 40, no. 5, pp. 795–800, 1992.
- [5] J. L. Hesler, K. Hui, and T. Crowe, "Analysis of an octagonal micromachined horn antenna for submillimeter-wave applications," *IEEE Transactions on Antennas and Propagation*, vol. 49, pp. 997–1001, June 2001.
- [6] F. Laermer and A. Schlip, "Method of anisotropically etching silicon," in *US Patent No. 5501893*.
- [7] E. Bassous, "Fabrication of novel three-dimensional microstructures by the anisotropic etching of (100) and (110) silicon," *IEEE Transactions on electron devices*, vol. 25, pp. 1178–1193, Oct. 1978.
- [8] M. Madou, *Fundamentals of Microfabrication - The Science of Miniaturation*, vol. ISBN 0-8493-0826-7. CRC Press, 2002.
- [9] T. J. Hubbard, *MEMS Design: The Geometry of Silicon Micromachining*. Ph.d. thesis, California Institute of Technology, Pasadena, CA, USA, 1994.
- [10] J. Schür, S. Biber, O. Cojocari, B. Mottet, L.-P. Schmidt, and H. L. Hartnagel, "600 GHz heterodyne mixer in waveguide technology using a GaAs Schottky diode," in *International Symposium on Space Terahertz Technology, Göteborg, Sweden*, 2005.